J. Phys. A: Math. Gen. 27 (1994) 3299–3321. Printed in the UK

Classical orbits and semiclassical wavepacket propagation in the Coulomb potential

I M Suárez Barnes†, M Nauenberg†, M Nockleby† and S Tomsovic†‡

† Institute of Nonlinear Sciences and Department of Physics, University of California, Santa Cruz, CA 95064, USA

‡ Department of Physics, FM-15, University of Washington, Seattle, WA 98195, USA

Received 26 January 1994

Abstract. A simple and elegant semiclassical theory for propagating wavepackets is presented. The development of the theory avoids the explicit use of the Green-function formalism. It involves expanding the potential to a quadratic time-dependent form and the use of multiple reference trajectories. The classical analogue in phase space predicts the accuracy of the results. The theory is applied to the calculation of the autocorrelation function in a Coulomb field in one dimension. Remarkable agreement with an exact quantum calculation is obtained in many circumstances in spite of the Coulomb singularity. All the detailed quantum behaviour, including the long-time recurrences and the spectrum, is reproduced.

1. Introduction

For many years, the stationary-phase approximation, known as time-dependent WKB (Wentzel–Kramers–Brillioun) [1], has been the standard semiclassical theory of quantum wavefunction propagation. It explains, in principle, how to evolve a quantum state approximately in terms of a predetermined set of classical trajectories. However in practice, implementations in non-trivial circumstances are difficult to find and guesses as to its accuracy have often been rather pessimistic. One available technique for propagating wavepackets semiclassically, has been linear wavepacket dynamics [2, 3]. However, this technique fails as soon as nonlinear classical dynamical behaviour arises; thus, often restricting the method to extremely short-time validity. The failure occurs whether the system is integrable or chaotic since both kinds of dynamics generically have nonlinearities. In the past couple of years, more sophisticated methods have been developed [4–10] and semiclassical propagation has proven to be surprisingly accurate even in fully developed chaotic situations [11–16]. These methods incorporate nonlinear dynamics through the use of a time-dependent semiclassical Green-function approach and multiple reference trajectories. Using these techniques as a guide, in recent work [17–19] we simplified this nonlinear dynamical theory by placing it in the same framework as earlier derivations of the linear wavepacket dynamics [2, 3]. Although this method is simpler in its approach and avoids the explicit use of Green functions, it leads to the same expressions for each reference trajectory's contribution to a correlation function as the Green-function work published in [14]. In this paper we give a full account of the semiclassical theory and also explore the classical–quantum correspondence by calculating the Wigner distribution and classical correlation function to the same level of approximation as our semiclassical method.

0305-4470/94/093299+23$19.50

Recent experimental advances [20–27] have created new possibilities for exploring the classical limit in atomic, molecular, and condensed-matter physics. However, much of the new progress with the semiclassical approximation has been made for simple models with little direct physical application. For this reason, we shall apply our method to the Coulomb potential, which is one of the most important cases for practical applications. A number of crucial points for such a case have been addressed in our previous work for the first time [17], where we have shown that: *(a)* semiclassical propagation is remarkably accurate in spite of the Coulomb singularity, *(b)* coherent quantum effects such as the already theoretically predicted and experimentally observed wavepacket recurrences and fractional recurrences [28–35] can be understood directly from a semiclassical *dynamical* point of view, i.e. without reference to the spectrum or WKB quantization of trajectories, *(c)* line intensities and discrete spectra are very well reproduced even though the trajectories involved span a continuous range of energies, *(d)* the circumstances under which our semiclassical method works can be determined in advance with the help of classical phase-space plots. Here we explain these and other issues in greater depth and investigate a wider variety of initial Gaussian wavepacket parameters than reported earlier. The quantum recurrence time is also calculated analytically from the semiclassical approximation, and a connection between the classical reference trajectories near the recurrence time and the Bohr orbits is established.

2. Extending wavepacket dynamics

As long as the natural wavelength of a problem is sufficiently small and a wavepacket is well localized in position and momentum, only the local behaviour of the potential in the neighbourhood of the wavepacket's moving centre is relevant to its evolution. The trajectory underlying the motion of the wavepacket's centre represents the local classical motion to within small linear deviations. All the neighbouring trajectories needed to construct the wavepacket are taken into account with a stability analysis of the central trajectory. This is how ordinary linear wavepacket dynamics works—one reference trajectory represents a group of trajectories that collectively fully support the construction of the evolving wavepacket [2, 3]. As nonlinearities in the dynamics begin to emerge, the wavepacket is no longer described by this single reference trajectory and its stability parameters. The purely classical dynamics is no longer being treated properly. The key to going beyond ordinary linear wavepacket dynamics as pointed out in [11–15] rests in restoring a proper treatment of the classical dynamics.

Taking the overlap of a localized wavepacket with the evolving wavefunction at time t can be used as a way of focusing or probing the information given by the classical phase space. It is thus helpful to consider such cross-correlation functions in generating our semiclassical theory. One of the most important in physical applications is the autocorrelation function, $C_\beta(t)$, which is measurable in pump–probe experiments [20–24, 31, 32]. For a localized wavepacket taken as the initial wavefunction, one has

$$C_\beta(t) = \langle\beta|\beta(t)\rangle = \int \mathrm{d}x \psi^*_\beta(x,0)\psi_\beta(x,t) \tag{1}$$

where β stands for the parameters (centre and variance of the wavepacket) that uniquely specify the initial state $\psi_\beta(x,0)$.

Using correlation functions considerably simplifies the job of incorporating nonlinear dynamics. Then a proper treatment of the nonlinear classical dynamics can be constructed by relying on multiple reference trajectories. The role of a reference trajectory is to represent a subclass of trajectories which are all extremely similar in their stability properties. In

general, the reference trajectories do not coincide with the position and momentum centroid of the wavepacket as does the trajectory at the heart of linear wavepacket dynamics. Such off-centre trajectories require some generalization, but are otherwise treated in the same way as the centred trajectories. At any given propagation time, the reference trajectories are selected in the local regions of the phase space which are physically relevant. For example, if a portion of the tail of the propagated wavepacket overlaps with the initial state, then the best reference trajectory originates from that tail, both in the position and momentum sense. Therefore the initial conditions of the reference trajectories are strongly time dependent, and the theory describes the choice of these reference trajectories as a function of time. With dynamics that is nonlinear, the need for multiple reference trajectories quickly develops whether the system is integrable or chaotic. Typically, the set of all contributing trajectories is easily separated into subgroups which appear as thin branches in the corresponding classical phase space. If the initial distribution is sufficiently localized, each branch is separate from the others, as can be seen from the classical phase-space figures which will be shown for the Coulomb problem in section 5. We will see that the number of collisions with the Coulomb singularity will uniquely label the branches. Each branch supports a local wavefront constructed as if it is part of an independent linearized wavepacket whose reference trajectory falls well within the part of the branch overlapping the initial state.

The coherent summation of the wavefronts gives the full semiclassical solution which is valid in the chosen region of phase space. Correlation functions are therefore written as sums over local solutions, one for each reference trajectory denoted by j. The autocorrelation function is

$$C_\beta(t) = \sum_j \langle \beta | \beta(t) \rangle_j \,. \tag{2}$$

The nonlinear dynamics now all resides in the summation, and a straightforward generalization of ordinary linear wavepacket dynamics will give the individual local solutions.

3. Selecting reference trajectories

Classical dynamics determines the appropriate set of reference trajectories. Roughly speaking, the phase-space portrait of a wavepacket can be deduced from its centroid and position and momentum uncertainties. Trajectories within elliptical phase-space domains having a volume a few times Planck's constant for each degree of freedom, are the most important. Reference trajectories outside this domain are Gaussian damped in the overlap integrals and do not contribute sufficiently to include them. By propagating just the outer boundary of the elliptical phase-space domain to a time t, the picture emerges as to the essential subgroups of trajectories that leave and return at t (see figures 1–3 below). A practical algorithm is needed to select one and only one reference trajectory centrally located within each branch.

One method of finding a suitable set of these reference trajectory points, which we describe and use below, is to locate the intersection points of two special trajectory manifolds. The details of implementation depend upon whether a system is integrable, where orbits shear away from each other, or chaotic, where orbits exponentially diverge in a locally hyperbolic way. In integrable systems, the interesting manifolds of initial conditions are those which sample points along different orbits (or rather different tori in multi-dimensions). For example, two initial conditions lying at different points along the same orbit give redundant information; there is no shearing between them. In a one-

dimensional system, the initial manifold is a line closely normal to the shear which passes through the centre of the initial wavepacket. It is propagated exactly a time t to give the final manifold. The intersections between the initial and final manifolds determine the reference trajectories completely. The manifold will have half the dimension of the phase space (the number of degrees of freedom, d). For systems with homogeneous potentials, i.e. $V(\alpha q) = \alpha^{\mu} V(q)$ (harmonic oscillator, billiards, Coulomb potential, etc), a further simplification arises. As the energy changes, the orbits only change in their scale. All orbits can be related back to an orbit on just one energy surface. This feature can be used to remove the search along the direction of maximal energy change in phase space which thus reduces the search to $(d-1)$-dimensional manifold intersections. The chaotic case has already been given [11–15]. There the special directions in phase space are determined by the local directions of stability (compression) and instability (stretching) and one finds heteroclinic orbit sums.

For the case of the initial decay of the propagated wavepacket away from the overlap region, it does not matter if the dynamics are chaotic or not. The reference trajectory may correspond to the mean position and mean momentum of the wavepacket as it is with ordinary linear wavepacket dynamics [2, 3]. In the neighbourhood of a severe nonlinearity (as is the case near the region of the Coulomb singularity) an improvement to this choice of reference trajectory can be made. A better choice is the trajectory that has the same energy as the trajectory corresponding to the mean momentum and mean position, but is half way in time between the initial centre of the wavepacket and the propagated centre of the wavepacket. This choice is closer to the point of maximal overlap between the initial and propagated states.

4. Wavefronts from reference trajectories

We now develop the semiclassical method to calculate the wavefunction associated with a particular reference trajectory and the corresponding individual term of the correlation function of (2). It begins by closely following [2]. For our purposes in later sections, the orbital angular momentum part of the Coulomb problem is of little interest and we can restrict ourselves to the one-dimensional Coulomb potential (or the case of zero angular momentum in three dimensions). In fact, zero angular momentum presents a serious difficulty because all trajectories collide with the singularity. We therefore develop the method in a one-dimensional notation though it should be clear that the multi-dimensional extension of most of the equations is straightforward. We reserve x to be our quantum configuration space variable and q, p (position, momentum respectively) to be our corresponding canonically conjugate phase-space variables.

The Schrödinger equation in one degree of freedom (in units where $\hbar$ and m are unity) is

$$\mathrm{i}\frac{\partial \psi(x,t)}{\partial t} = -\frac{1}{2}\frac{\partial^2 \psi(x,t)}{\partial x^2} + V(x)\psi(x,t) \tag{3}$$

where $V(x)$ is the potential. Let us assume that we are interested in the local approximation associated with one particular reference trajectory which is specified by its collection of position and momentum values for all times which we denote $\{q_t, p_t\}$. We presume that the trajectory satisfies the equations of motion for the corresponding classical Hamiltonian, $H = p_t^2/2 + V(q_t)$. A solution of (3) best suited to the neighbourhood of such a trajectory starts by expanding the potential $V(x)$ about q_t up to the quadratic form

$$V(x) = V(q_t) + V'(q_t)(x - q_t) + \tfrac{1}{2}V''(q_t)(x - q_t)^2 . \tag{4}$$

Since q_t is evolving, the expansion is continuously changing with time.

Suppose that at $t = 0$, the wavefunction $\psi_\beta(x, 0)$ is a Gaussian. Equations (3) and (4) govern the motion of a quantum harmonic oscillator with time-varying frequency and centre. Therefore, any initial state with a Gaussian or wavepacket form will, under evolution, always retain a Gaussian form, albeit distorted. We may therefore express the solution as

$$\psi_\beta(x, t) = A \exp\{i[\xi_t(x - q_t) + \alpha_t(x - q_t)^2 + \gamma_t]\}. \tag{5}$$

The variables ξ_t, α_t and γ_t are complex functions depending on time and the initial conditions β. The normalization factor A is time independent. Substitution of the Gaussian wavefunction (5) and the approximate potential (4) into Schrödinger's equation and equating the coefficients of like powers of $(x - q_t)$ yields the ordinary differential equations

$$\begin{aligned} &\dot{\alpha}_t = -2\alpha_t^2 - \tfrac{1}{2}V''(q_t) \qquad \dot{\gamma}_t = \xi_t\dot{q}_t - \tfrac{1}{2}\xi_t^2 - V(q_t) + i\alpha_t \\ &\dot{\xi}_t = 2\alpha_t\dot{q}_t - 2\alpha_t\xi_t - V'(q_t) \end{aligned} \tag{6}$$

where q_t and p_t satisfy the classical Hamiltonian equations of motion

$$\dot{q}_t = p_t \qquad \dot{p}_t = -V'(q_t). \tag{7}$$

A few substitutions in (6) considerably simplify finding their solutions. The first equation of (6) can be solved by assuming that α_t has the form

$$\alpha_t = \frac{f_t}{2g_t} \tag{8}$$

where g_t and f_t satisfy the linear equations

$$\dot{g}_t = f_t \qquad \dot{f}_t = -V''(q_t)g_t. \tag{9}$$

Equations (7) and (9) indicate that g_t and f_t correspond to first-order variations of the coordinates q_t and p_t. Setting $\xi_t = p_t + \zeta_t$, generates the equations

$$\dot{\zeta}_t = -2\alpha_t\zeta_t \qquad \dot{\gamma}_t = L + i\alpha_t - \frac{\zeta_t^2}{2} \tag{10}$$

where $L = p_t^2/2 - V(q_t)$ is the classical Lagrangian.

In order to integrate (10), we need to find the integral of α_t with respect to time;

$$\int_0^t \alpha_{t'}\,dt' = \frac{1}{2}\int_0^t \frac{\dot{g}_{t'}}{g_{t'}}\,dt' = \frac{1}{2}\ln(g_t) \tag{11}$$

where we have chosen $g_0 = 1$. Then the solution of the first equation of (10) takes the form

$$\zeta_t = \frac{\zeta_0}{g_t} \tag{12}$$

where ζ_0 is a constant determined by the initial conditions. Therefore, the second equation of (10) becomes

$$\dot{\gamma}_t = L + i\alpha_t - \frac{\zeta_0^2}{2g_t^2}. \tag{13}$$

Integrating the last term on the right-hand side of (13) we find

$$\int_0^t \frac{1}{g_{t'}^2}\,dt = \frac{g^{(h)}}{g_t} \tag{14}$$

where $g^{(h)}$ is a particular solution to the first equation of (9) and satisfies that the Wronskian $W(g_t, g^{(h)}) = 1$. Therefore, $g^{(h)}(0) = 0$ and $\dot{g}^{(h)}(0) = 1$ and the solution of (13) is

$$\gamma_t = \gamma_0 + S + \frac{i\ln g_t}{2} - \frac{\zeta_0^2 g^{(h)}}{2g_t} \tag{15}$$

where $S = \int_0^t L\mathrm{d}t'$ is the classical action.

A unit-normalized initial Gaussian wavepacket of variance σ_β^2, centred at q^β and with average momentum of p^β, has the form

$$\psi_\beta(x,0) = (\pi\sigma_\beta^2)^{-1/4}\exp\left[\mathrm{i}p^\beta(x-q^\beta) - \frac{(x-q^\beta)^2}{2\sigma_\beta^2}\right]. \tag{16}$$

Comparing to the notation of (5), we obtain at $t = 0$

$$\alpha_0 = \mathrm{i}/2\sigma_\beta^2 \qquad \gamma_0 = (q_0 - q^\beta)[\alpha_0(q_0 - q^\beta) + p^\beta] \qquad \xi_0 = p^\beta + 2\alpha_0(q_0 - q^\beta) \tag{17}$$

and $A = (\pi\sigma_\beta^2)^{-1/4}$. Setting $g_0 = 1$, implies that ζ_0 in (12) is

$$\zeta_0 = \xi_0 - p_0 = 2\alpha_0(q_0 - q^\beta) + p^\beta - p_0\,. \tag{18}$$

Therefore,

$$\xi_t = p_t + \frac{2\alpha_0(q_0 - q^\beta) + p^\beta - p_0}{g_t}. \tag{19}$$

Finally, substituting the initial Gaussian wavepacket $\psi_\beta(x,0)$ and the propagated wavepacket $\psi_\beta(x,t)$, both given by (5), into $\langle\beta|\beta(t)\rangle_j$, we find an individual term of the autocorrelation function to be

$$\langle\beta|\beta(t)\rangle_j = \left\{\left(\frac{2\alpha_0}{\alpha_t+\alpha_0}\right)^{1/2}\exp\left[\mathrm{i}(\gamma_t - \gamma_0^*) - \frac{\mathrm{i}(\xi_t - \xi_0^*)^2}{4(\alpha_t+\alpha_0)} + \frac{\mathrm{i}(\alpha_t\xi_0^* + \alpha_0\xi_t)(q_0 - q_t) + \mathrm{i}\alpha_t\alpha_0(q_0 - q_t)^2)}{(\alpha_t+\alpha_0)}\right]\right\}_j \tag{20}$$

where j labels the particular reference trajectory $\{q_t, p_t\}_j$, and α_t, γ_t, and ξ_t are given by (8), (15) and (19) and α_0, γ_0, and ξ_0 are given by (17), all evaluated for each particular reference trajectory. Depending on the particular form of the potential $V(x)$, the functions g_t, f_t, and $g^{(h)}$ are obtained by solving (9). Exactly the same result is obtained using the Green-function approach [14]†. It should be noted that $\langle\beta|\beta(t)\rangle_j$ depends on $\exp(\mathrm{i}\gamma_t)$ (see (20)) which in turn is proportional to $g_t^{-1/2}$. Although the square root is double-valued, the appropiate branch is generally obtained by the requirement that the phase must evolve continuously with time. However, for the case of the Coulomb potential which is singular at the origin, g_t vanishes when the reference trajectory crosses this point, and it is then not possible to fix the phase by this continuity argument. We have found that this phase is unity, but this requires mathematical justification.

For the special case that $q_t = q_0$, equation (20) simplifies considerably to the special form

$$\langle\beta|\beta(t)\rangle_j = \left\{\left(\frac{2\alpha_0}{\alpha_t+\alpha_0}\right)^{1/2}\exp\left[\mathrm{i}(\gamma_t - \gamma_0^*) - \frac{\mathrm{i}(\xi_t - \xi_0^*)^2}{4(\alpha_t+\alpha_0)}\right]\right\}_j. \tag{21}$$

To obtain the full autocorrelation function $C_\beta(t)$ of (2), a summation over reference trajectories j is made where the individual terms are given by (20) (or (21) if $q_t = q_0$).

† To make detailed comparison between (20) and the formulae given in [14, 15], note that f_t,g_t, and $g^{(h)}$ can be written in terms of stability matrix elements M_{ij}: $f_t = 2\alpha_0 M_{11} + M_{12}$, $g_t = 2\alpha_0 M_{21} + M_{22}$, and $g_{(h)} = M_{21}$; see also [19].

5. Coulomb Potential

For the one-dimensional Coulomb potential $V(q) = -1/q$ where $q > 0$, the classical equations of motion can be solved in parametric form, with

$$q_t = \frac{1}{2E}(1-\cos\theta) \qquad p_t = (2E)^{1/2}\frac{\sin\theta}{(1-\cos\theta)} \tag{22}$$

where θ is implicitly determined by the time t

$$t = \frac{1}{(2E)^{3/2}}(\theta - \sin\theta) + t_0 \tag{23}$$

$E = 1/q_0 - p_0^2/2$ is the magnitude of the Kepler energy for the bound orbit starting at (q_0, p_0), and the constant t_0 is determined by what θ is at $t = 0$. Therefore, the solutions to (9) are

$$\begin{aligned} g_t &= \frac{\alpha_0}{E}(2p_0q_t - 2q_0p_t - 3tp_0p_t) + \frac{1}{2q_0^2E}(2q_t - 3tp_t - q_0^2p_0p_t) \\ f_t &= \frac{1}{q_t^2E}\left[\alpha_0(3tp_0 + 2q_0 - q_t^2p_0p_t) + \frac{1}{2q_0^2}(3t + p_0q_0^2 - q_t^2p_t)\right] \end{aligned} \tag{24}$$

where the initial conditions have been chosen to be $g_0 = 1$ and $f_0 = 2\alpha_0 = \mathrm{i}/\sigma_\beta^2$ (see details in appendix A). The particular solution $g^{(h)}$ to the first equation of (9) is

$$g^{(h)} = \frac{1}{2E}(2p_0q_t - 2q_0p_t - 3tp_0p_t) \tag{25}$$

(see appendix A). The classical action for the Coulomb potential is

$$S = 3Et + 2(q_tp_t - q_0p_0)\,. \tag{26}$$

We can now calculate α_t, γ_t, and ξ_t from (8), (15) and (19) and then substitute them in (20) to obtain an individual term of the autocorrelation function associated with the classical reference trajectory q_t, p_t.

In what follows, we are going to simplify many of our calculations by choosing the initial wavepacket $\psi_\beta(x, 0)$ of (16) to be centred at the outer classical turning point of the Coulomb potential, so that $q^\beta = 1/E_\beta$ and $p^\beta = 0$. The initial variance of this Gaussian wavepacket is σ_β^2. The Kepler period of the centre of the Gaussian is $\tau_\beta = 2\pi/(2E_\beta)^{3/2}$.

To evaluate the autocorrelation function for the Coulomb potential, a suitable set of reference trajectories must be chosen. We want a reference trajectory at time t to be at a point in phase space that is close to the maximal overlap between the initial and propagated wavepackets. The initial decay of the wavepacket for $t < \tau_\beta/2$ and the recurrences of the wavepacket for $t > \tau_\beta/2$ must be handled separately.

For the case of the initial decay, a good choice for a reference trajectory is the trajectory that is about halfway between the initial centre of the wavepacket q^β and the propagated centre of the packet after a time t (kept $< \tau_\beta/2$) in phase space. Figure 1 shows a contour in phase space of the initial Gaussian wavepacket and the contour of its propagated state after a time $t < \tau_\beta/2$. The points on the initial contour are propagated forward to time t by the classical equations of motion. The centre of the Gaussian has an energy of E_β and starts at $(q^\beta, p^\beta) = (1/E_\beta, 0)$. During a time interval $t < \tau_\beta/2$, a classical trajectory with the same energy E_β that starts at a point (q_c, p_c) is propagated to its image point $(q_c, -p_c)$. This point is near the maximal overlap between the initial and propagated states, which ensures an accurate approximation to the autocorrelation function when used as a reference trajectory for the initial decay. This choice of reference trajectory also has the advantages

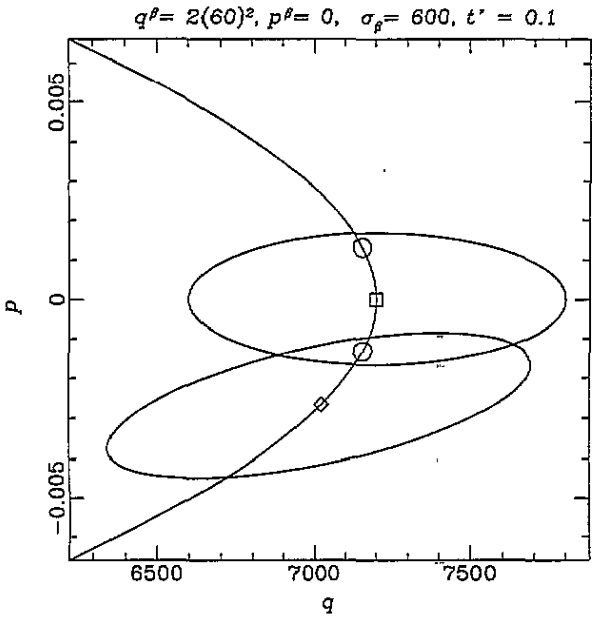

Figure 1. An ellipse in phase space representing a 1σ contour of the initial Gaussian with parameters $q^\beta, p^\beta, \sigma_\beta$ is propagated classically to a time $t' = 0.1$. The centres of the initial and propagated ellipses are denoted by □. The reference trajectory has the same energy $E_\beta = 1/q^\beta$ as the centre of the wavepacket and starts at (q_c, p_c) and lands at $(q_c, -p_c)$ (both denoted by ○). The point of maximal overlap between the initial and propagated wavepackets is near $(q_c, -p_c)$.

of staying away from the Coulomb singularity and that the calculations simplify somewhat due to the symmetry between the two points $(q_0, p_0) = (q_c, p_c)$ and $(q_t, p_t) = (q_c, -p_c)$. Note that both the initial and final conditions of the reference trajectory change with time as the autocorrelation function is evaluated. These constraints given by our choice of reference trajectory yield the relations $\theta = \theta_c$ at $t = 0$ and $\theta = 2\pi - \theta_c$ at time t. Therefore from (23) (where $t_0 = (-\theta_c + \sin\theta_c)/(2E_\beta)^{3/2}$), we obtain

$$t = \frac{2}{(2E_\beta)^{3/2}}(\pi - \theta_c + \sin\theta_c) \tag{27}$$

which is solved numerically to find θ_c. Also q_c and p_c can be evaluated at θ_c using (22). Then from (24) we obtain

$$\begin{aligned} g_t &= \frac{\alpha_0}{E_\beta}(4p_cq_c + 3tp_c^2) + \frac{1}{2q_c^2E_\beta}(2q_c + 3tp_c + q_c^2p_c^2) \\ f_t &= \frac{1}{q_c^2E_\beta}\left[\alpha_0(3tp_c + 2q_c + q_c^2p_c^2) + \frac{1}{2q_c^2}(3t + 2q_c^2p_c)\right] \end{aligned} \tag{28}$$

where $\alpha_0 = i/2\sigma_\beta^2$ and $E_\beta = 1/q^\beta$. From (25) and (26) we obtain

$$g^{(h)} = \frac{1}{2E_\beta}(4p_cq_c + 3tp_c^2) \tag{29}$$

$$S = 3E_\beta t - 4q_cp_c. \tag{30}$$

Using (28)–(30) we can calculate α_t, γ_t, and ξ_t from equations (8), (15) and (19) respectively, where $q_t = q_c$, $p_t = -p_c$, and the initial conditions α_0, γ_0, and ξ_0 are given by (17) where $q_0 = q_c$, $p_0 = p_c$, and $p^\beta = 0$. Since $q_t = q_0$, the autocorrelation function for the initial decay is given by (21), where the sum over trajectories in (2) reduces to one term given by the reference trajectory defined by (q_c, p_c).

When we continue the approximation for times greater than half the Kepler period of the central trajectory, we soon find that the propagated state has more than one contribution,

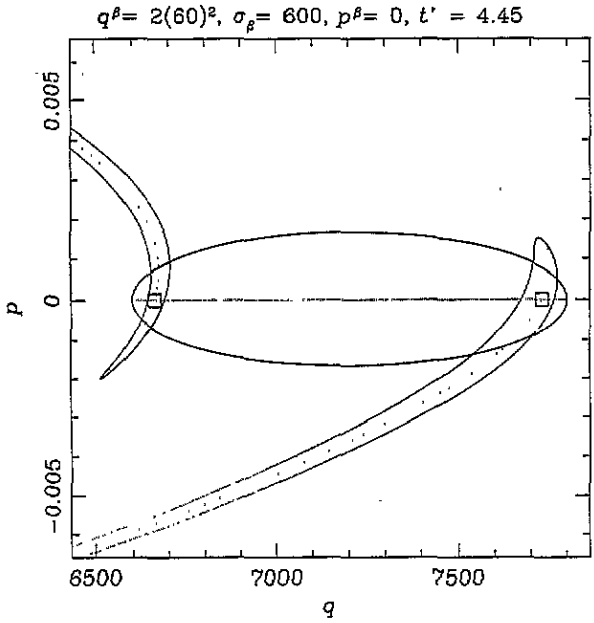

Figure 2. An ellipse in phase space representing a 1σ contour of the initial Gaussian with parameters $q^\beta, p^\beta, \sigma_\beta$ is propagated classically to a time $t = 4.45$. The inner branch is formed by trajectories on their fifth return, and the outer branch are those on their fourth return. The initial manifold ($p = 0$ curve inside ellipse) is likewise propagated to give the final manifold (dotted curve), and the intersections correspond to the initial and final points (denoted by □) of the reference trajectories used to calculate the autocorrelation function.

as the leading edge of the propagated wavepacket has travelled around the Coulomb centre more times than the trailing edge. We choose the initial manifold as the q axis in phase space, which in this case is normal to the flow in phase space and passes through the centre of the initial wavepacket. This manifold is propagated after a time t to give the final manifold. The intersections between the two manifolds determine the set of reference trajectories. Therefore, the reference trajectories are given by the periodic points along the q axis in phase space at a time $t > \tau_\beta/2$. Figure 2 illustrates the procedure for an initial state centred on the q axis, which has propagated into two contributions after a time t (now considering $> \tau_\beta/2$). The leading edge has travelled around the Coulomb singularity once more than the trailing edge. The initial manifold along the q axis has evolved into the final manifold to give the intersections which are near the areas of maximal overlap between the final and initial states. The periodic points which correspond to our choice of reference trajectories follow the points of maximum overlap between the initial wavepacket and the propagated wavepackets as time passes, as illustrated by figure 3. These points are simple to obtain, one has only to tune the energies of the periodic points such that they close at exactly time t.

Let the jth periodic point be denoted $(q_j, 0)$. Then $(q_0, p_0) = (q_t, p_t) = (q_j, 0)$. The periodic orbits will return to the starting classical turning points q_j which are given by

$$q_j = \left(\frac{t}{j\tau_\beta}\right)^{2/3} q^\beta = \left(\frac{t'}{j}\right)^{2/3} q^\beta \tag{31}$$

where $t' = t/\tau_\beta$ is the time in units of the Kepler period τ_β of the central trajectory and j is the number of times the periodic orbit has returned to the classical turning point during time t'. Such periodic orbits have an energy $E_j = 1/q_j$ and a period $\tau_j = 2\pi/(2E_j)^{3/2}$, and so $j\tau_j = t = t'\tau_\beta$. Therefore, the correlation function for $t' > 0.5$ is given by (21) where we calculate every time-dependent quantity by setting $q_t = q_0 = q_j$ and $p_t = p_0 = p_j = 0$. Thus, from (24)–(26), we obtain: $g_t = 1$, $f_t = 2\alpha_0 + 3\tau_\beta j^2/(2q^{[\beta]3}t')$, $g^{(h)} = 0$, and

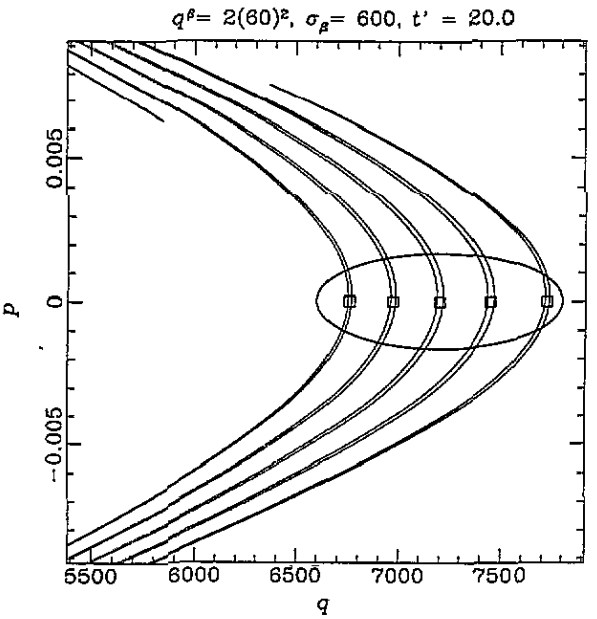

Figure 3. The initial and classically propagated wavepackets in phase space when $t' = 20.0$. The initial ellipse is defined by the 1σ contour and the periodic points along the q axis which correspond to the reference trajectories are denoted by boxes. These periodic points corresponding to the reference trajectories are denoted by boxes. These periodic points have travelled around the Coulomb singularity 18, 19, 20, 21, and 22 times from right to left, respectively.

$S = 3\tau_\beta (j^2 t')^{1/3}/q^\beta$. Using (8), (15), (17) and (19), the quantities in (21) are given by

$$(\xi_t - \xi_0^*)_j = 4\alpha_0 q^\beta \left[\left(\frac{t'}{j}\right)^{2/3} - 1\right] \qquad (\alpha_t + \alpha_0)_j = 2\alpha_0 + \frac{3\tau_\beta j^2}{4q^{[\beta]3}t'}$$
$$(\gamma_t - \gamma_0^*)_j = \frac{3\tau_\beta}{q^\beta}(j^2 t')^{1/3} + 2\alpha_0 q^{[\beta]2}\left[\left(\frac{t'}{j}\right)^{2/3} - 1\right]^2 \tag{32}$$

where $\alpha_0 = \mathrm{i}/2\sigma_\beta^2$. We find that the autocorrelation function (excluding the initial decay) for an initial Gaussian wavepacket centred around the turning point $q^\beta = 1/E_\beta$ and the variance σ_β^2 is

$$C_\beta(t) = \sum_{j=1}^{\infty}\left(\frac{t'}{t' + \mu_\beta j^2}\right)^{1/2} \exp\left\{\mathrm{i}\frac{3\tau_\beta}{q^\beta}(j^2 t')^{1/3} + \mathrm{i}\frac{2\alpha_0 \mu_\beta q^{[\beta]2} j^2[(t'/j)^{2/3} - 1]^2}{(t' + \mu_\beta j^2)}\right\} \tag{33}$$

where $\mu_\beta = 3\tau_\beta/8\alpha_0 q^{[\beta]3}$ is a purely imaginary unitless quantity. Note that the major contributions in the sum come from the jth terms where j is close to t'.

We now compare the autocorrelation function obtained with our semiclassical method and that obtained from an exact quantum calculation (see appendix B) for the case where $q^\beta = 7200$ and $\sigma_\beta = 600$. This is very close to experimentally realizable wavepackets [20–24, 31, 32]. In this case the central orbit corresponds to a quantum number of $n = 60$. Figure 4 illustrates the excellent agreement between the real parts of the semiclassical and quantum autocorrelation functions for the initial decay and first recurrence of the Gaussian wavepacket. The comparison between the semiclassical and quantum autocorrelation functions is extended to 10 and 25 Kepler periods of the central trajectory by plotting the absolute values of the autocorrelation function in figures 5 and 6, respectively.

In addition to the autocorrelation function, the semiclassical approximation accurately reproduces the quantum spectrum. The Fourier transform of $C_\beta(t)$ gives the intensity weighted spectrum,

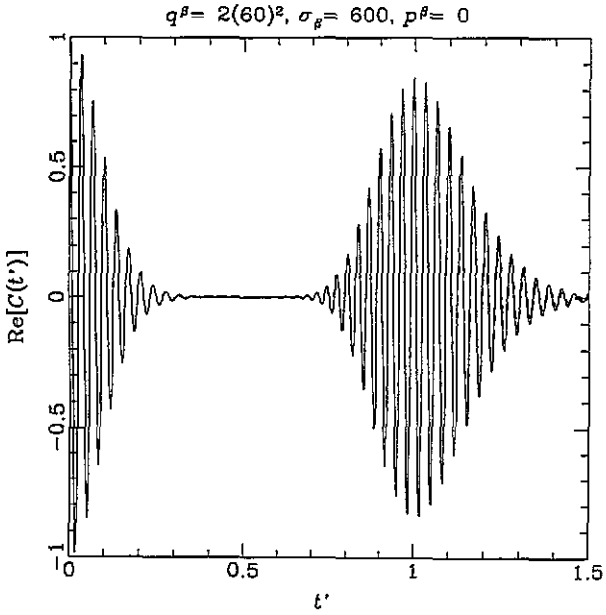

Figure 4. A comparison of the real part of the semiclassical (full curve) and the real part of quantum (broken curve) autocorrelation functions $C_\beta(t')$, where $q^\beta = 7200$ and $\sigma_\beta = 600$ for the initial decay and initial recurrence of the Gaussian wavepacket.

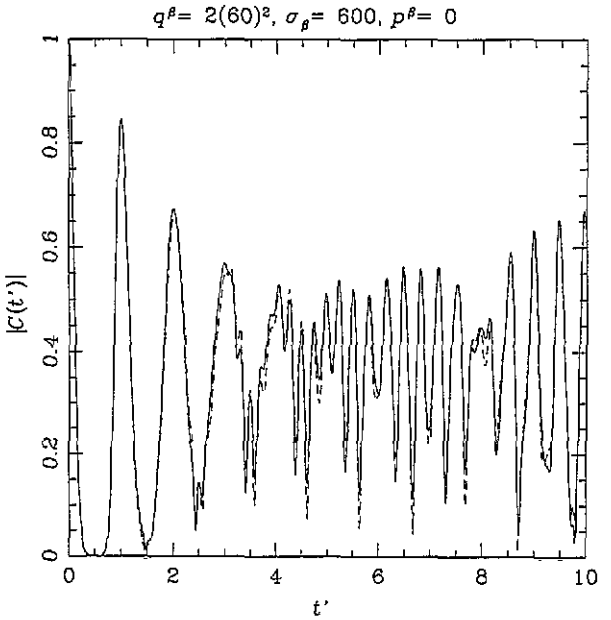

Figure 5. A comparison of the absolute value of the semiclassical (full curve) and quantum (broken curve) autocorrelation functions $C_\beta(t')$, where $q^\beta = 7200$ and $\sigma_\beta = 600$ for the first 10 Kepler periods of the centre of the Gaussian wavepacket.

$$S(E) = \int dt \exp(iEt) C_\beta(t) \tag{34}$$

and figure 7 shows the comparison with the exact spectrum, given by

$$S(E) = \sum |\langle \beta | E_n \rangle|^2 \delta(E - E_n). \tag{35}$$

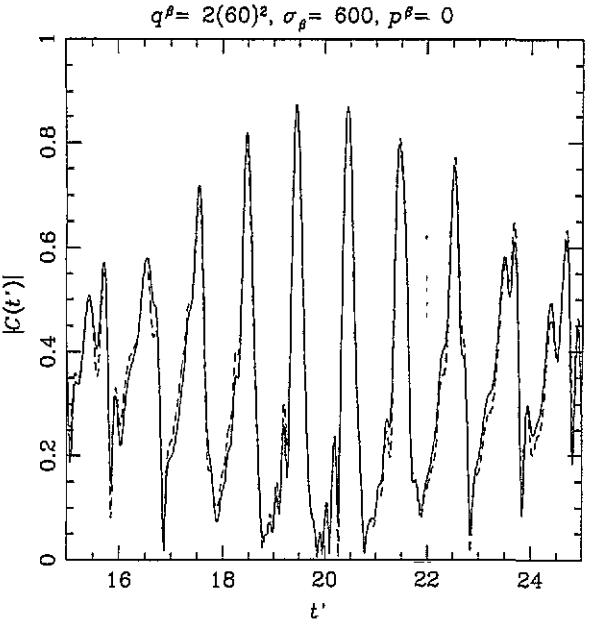

Figure 6. A comparison of the absolute value of the semiclassical (full curve) and quantum (broken curve) autocorrelation functions $C_\beta(t')$, where $q^\beta = 7200$ and $\sigma_\beta = 600$ for the 10 Kepler periods between 15 and 25 Kepler periods of the central orbit. Notice that the full quantum recurrences of the wavepacket, at approximately $n/3 = 20$, are accurately described.

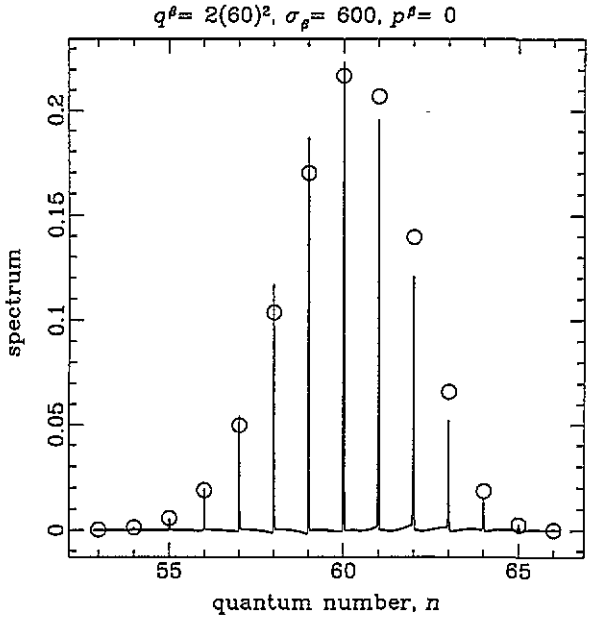

Figure 7. A comparison between the semiclassical (full curve) and quantum (circles) spectra for the case of $q^\beta = 7200$ and $\sigma_\beta = 600$.

Plotting the spectrum computed with a finite time resolution of 50 Kepler periods vs the 'quantum number' $n = (2E)^{-1/2}$ in figure 7 shows that the peaks occur very accurately at integer values of n, as expected for the Coulomb potential, and the intensities are within $\pm 5\%$ of the exact values. This remarkable reproduction of the familiar quantum spectrum of the Coulomb is obtained with classical reference trajectories that have a continuous energy range. No quantization conditions on the actions of the classical reference trajectories are imposed as they are with standard WKB quantization. Indeed, standard WKB quantization is not valid here due to the Coulomb singularity at the origin, and it gives an incorrect

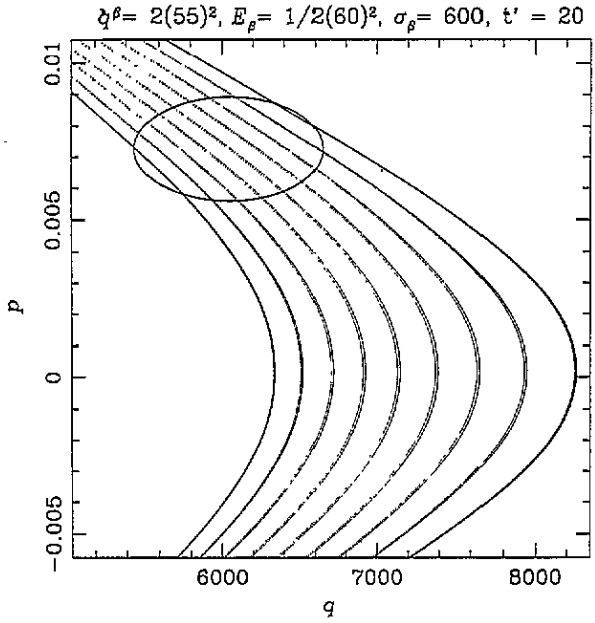

Figure 8. The initial and classically-propagated wavepackets in phase space when $t' = 20.0$ for the case where the initial wavepacket is not at the classical turning point.

spectrum [36].

For the case where the initial Gaussian wavepacket has a non-zero average momentum, the agreement between the semiclassical and quantum autocorrelations is better than the case when $p^\beta = 0$. In this case, the initial wavepacket is away from the classical turning point. Near this point, there is a high degree of curvature in the classical manifolds in phase space. Because the classical trajectories form straight lines away from the classical turning point (see figure 8), the wavepackets are more easily modelled with linear Gaussian approximations. The reference trajectories for such a wavepacket are similar to the reference trajectories for the initial wavepacket at the classical turning point. The reference trajectories for the initial decay ($t < \tau_\beta/2$) of the autocorrelation function have the same energy as the central trajectory of the Gaussian wavepacket. The coordinates (p_0, q_0) and (p_t, q_t) are such that it takes $t/2$ to propagate from (p_0, q_0) to (p_β, q_β) and $t/2$ to propagate from (p_β, q_β) to (p_t, q_t), just as it does for the case where $p_\beta = 0$. For $t > \tau_\beta/2$, multiple trajectories are used. For this case, the initial manifold in the phase space is taken to be the constant momentum line at p_β. The reference trajectories are the points that return to this line after a time t. The periods of the reference trajectories are related to the period of the central trajectory as before, $j\tau_j = t = t'\tau_\beta$, where $\tau_j = 2\pi/(2E_j)^{3/2}$ and $E_j = 1/q_j - p_\beta^2/2$. Therefore, the reference trajectories are given by

$$(p_0, q_0) = (p_j, q_j) = \left(p_\beta, \left[E_\beta\left(\frac{j}{t'}\right)^{2/3} + \frac{p_\beta^2}{2}\right]^{-1}\right) \tag{36}$$

where j is the number of collisions with the Coulomb singularity. Once the reference trajectories are found, the autocorrelation function is then calculated with (21). Figure 8 illustrates the propagation in phase space of a non-zero average-momentum wavepacket. The corresponding comparison between the semiclassical autocorrelation and the quantum correlation is shown in figure 9.

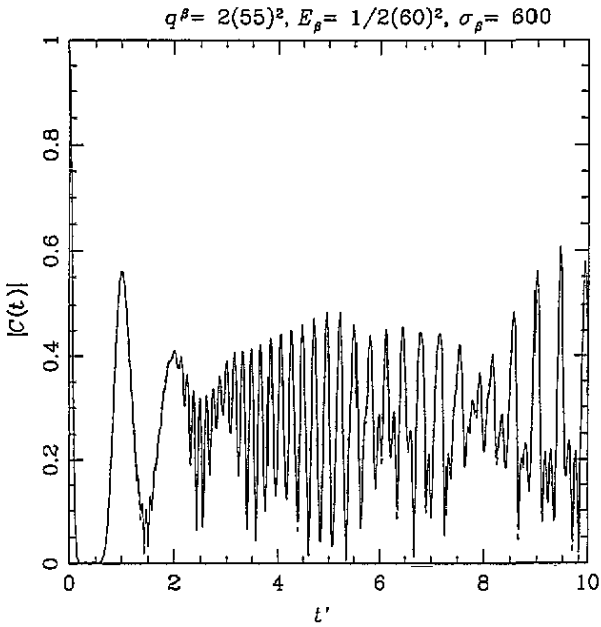

Figure 9. A comparison of the absolute value of the semiclassical (full curve) and quantum (broken curve) autocorrelation functions $C_\beta(t')$, where $E_\beta = \frac{1}{2}(60)^2$, $q^\beta = 6050$ and $\sigma_\beta = 600$ for the first 10 Kepler periods of the centre of the Gaussian wavepacket.

6. Wavepacket recurrences

In integrable systems, wavepackets recur after a well defined time [28–34]. This recurrence time can be calculated from the semiclassical approximation. When a recurrence occurs, each contribution to the autocorrelation function corresponding to a classical reference trajectory should add constructively. In other words, at the recurrence time each contributing phase to the autocorrelation function should be nearly equal (mod 2π). The dominant time-dependent phase in the autocorrelation function of (33) is

$$\phi_j = \frac{3\tau_\beta}{q^\beta}(j^2 t')^{1/3}. \tag{37}$$

Expanding the phase factor to second order in $k = j - N$, where N is the nearest integer to t, and substituting for $\tau_\beta/q^\beta = 2\pi(q^\beta/2)^{1/2}$ yields

$$\phi_j - \phi_N \simeq 2\pi k \left(\frac{q^\beta}{2}\right)^{1/2} \left(\frac{t'}{N}\right)^{1/3} \left(1 - \frac{k}{6N}\right). \tag{38}$$

Classically, we can express the centre of the initial Gaussian wavepacket as $q_\beta = 2(n_\beta + f)^2$, where n_β is an integer and $-\frac{1}{2} \leqslant f \leqslant \frac{1}{2}$. Then (38) at time $t' = N - f + \delta$ becomes

$$\phi_j - \phi_N \simeq 2\pi k \left(n_\beta + f\right) \left(1 + \frac{\delta - f}{N}\right)^{1/3} \left(1 - \frac{k}{6N}\right) \tag{39}$$

where N is the nearest integer to $n_\beta/3$, and δ is an undetermined small parameter. Expanding (39) up to quadratic order in f, k and δ gives

$$\phi_j - \phi_N \simeq 2\pi k \left[n_\beta + (\delta - k/2)\left(n_\beta/3N\right) + f\left(1 - n_\beta/3N\right)\right]. \tag{40}$$

For large quantum number, $n_\beta/3N$ can be taken to be unity, and then if $\delta = \pm\frac{1}{2}$ the difference in the phases corresponding to adjacent reference trajectories is an integer multiple of 2π and the initial wavepacket reforms at a time $t' = N - f \pm \frac{1}{2}$. Furthermore, if $\delta = 0$

in (40), then destructive interference between each contribution occurs at $t' = N - f$, as the relative phase difference between adjacent contributions is π. A full recurrence of the wavepacket is illustrated in figure 6, which for $n_p = 60$ occurs at $t' = 20 \pm 1/2$.

As time passes in the region of the initial localized wavepacket, the reference trajectories continuously shift towards the origin and become more densely spaced. Near the recurrence time, the spacing of the reference trajectories is close to the spacing of the Bohr orbits. At a special time, the classical reference trajectories nearly coincide with the Bohr orbits. The difference between q^β and nearby Bohr orbits is given by

$$q^\beta - 2(n_\beta - k)^2 = 4n_\beta(f + k) + 2(f^2 - k^2) \tag{41}$$

where k is a small integer labelling the nearby Bohr orbits. Now let us examine the difference between q^β and nearby reference trajectories $q_j \simeq q^\beta(t/j)^{2/3}$ at a time $t' = N - f$,

$$q^\beta - q_j = q^\beta \left[1 - \left(\frac{1 - f/N}{1 + k/N} \right)^{2/3} \right] \tag{42}$$

where $k = j - N$, and N is the nearest integer to $n_\beta/3$ as before. Expanding (42) to first order in f and k yields

$$q^\beta - q_j \simeq 4n_\beta(f + k)\left(n_\beta/3N\right). \tag{43}$$

If the quantum number n_β is large, then the factor $n_\beta/3N$ is close to unity. Comparing (43) with (41) shows that to first order the classical reference trajectories coincide with the Bohr orbits near the time when the wavepacket reconstructs itself.

7. Wigner distribution and the classical probability

Further insight into the classical–quantum correspondence is gained by calculating the Wigner distribution and the classical probability function to the same level of approximation as our semiclassical method. The classical phase-space distribution analogous to the quantum wavepackets is given by the Wigner probability distribution [37–39]

$$F_w(x, p, t) = (2\pi)^{-1/2} \int \psi^*(x - y/2, t) \exp(-\mathrm{i}py)\psi(x + y/2, t)\,\mathrm{d}y \tag{44}$$

which is positive definite for the case of a Gaussian wavepacket. Upon substituting the wavefunction

$$\psi(x, t) = A \exp\{\mathrm{i}[(p_t + \zeta_t)(x - q_t) + \alpha_t(x - q_t)^2 + \gamma_t]\} \tag{45}$$

into (44), the Wigner function takes the general form of

$$\begin{aligned} F_w(x, p, t) = A_t \exp\{&a_t(x - q_t)^2 + b_t(p - p_t)^2 + c_t(x - q_t)(p - p_t) \\ &+ d_t(x - q_t) + e_t(p - p_t)\}, \end{aligned} \tag{46}$$

where

$$\begin{aligned} A_t &= |A|^2 (\mathrm{Im}\,\alpha_t)^{-1/2} \exp\left(-2\mathrm{Im}\,\gamma_t - \frac{(\mathrm{Re}\,\zeta_t)^2}{2\mathrm{Im}\,\alpha_t} \right) \\ a_t &= -\frac{2|\alpha_t|^2}{\mathrm{Im}\,\alpha_t} \qquad b_t = -\frac{1}{2\mathrm{Im}\,\alpha_t} \qquad c_t = \frac{2\mathrm{Re}\,\alpha_t}{\mathrm{Im}\,\alpha_t} \\ d_t &= -2\left(\mathrm{Im}\,\zeta_t + \frac{\mathrm{Re}(\zeta_t)\mathrm{Re}(\alpha_t)}{\mathrm{Im}\,\alpha_t} \right) \qquad e_t = +\frac{\mathrm{Re}\,\zeta_t}{\mathrm{Im}\,\alpha_t}. \end{aligned} \tag{47}$$

In the limit $h \to 0$, the Wigner probability distribution satisfies the Liouville equation

$$\frac{\partial F_w}{\partial t} + \frac{\partial F_w}{\partial x} p - \frac{\partial F_w}{\partial p} V'(x) = 0 . \tag{48}$$

Substituting (46) into the Liouville equation and expanding the potential to quadratic order about a reference trajectory q_t

$$V(x) = V(q_t) + V'(q_t)(x - q_t) + \tfrac{1}{2} V''(q_t)(x - q_t)^2 \tag{49}$$

as we did with Schrödinger's equation, generates the following differential equations (obtained by equating coefficients of like powers of $(x - q_t)(p - p_t)$):

$$\begin{aligned} &\dot{A}_t = 0 \qquad \dot{a}_t = c_t V''(q_t) \qquad \dot{b}_t = -c_t \\ &\dot{c}_t = -2a_t + b_t V''(q_t) \qquad \dot{d}_t = e_t V''(q_t) \qquad \dot{e}_t = -d_t . \end{aligned} \tag{50}$$

If the time evolution of q_t, p_t, ξ_t, α_t, and γ_t in (47) are given by the ordinary differential equations derived in the semiclassical approximation (equations (6), (7) and (10)), then (47) are solutions to the differential equations derived from the Wigner function (50) as well. For instance, substituting the semiclassical solutions to α_t, γ_t, and ξ_t into the first of (47) gives $A_t = (2/\pi)^{1/2} \exp[-(q^\beta - q_0)^2 - \sigma_\beta^2 (p^\beta - p_0)^2]$ which is indeed a constant. In this way, the classical probability function associated with each reference trajectory (q_t, p_t) is equal to the square of an individual term of the semiclassical autocorrelation function

$$\int F_w(x, p, t) F_w(x, p, 0)\, dx\, dp = |\langle \beta | \beta(t) \rangle_j|^2 . \tag{51}$$

In calculating the total classical probability function $P_\beta(t)$ the phase information associated with each reference trajectory is absent in the summation of the terms for each reference trajectory. Therefore, adding the terms associated with each reference trajectory together gives an incoherent sum, where there is no interference between the individual terms

$$P_\beta(t) = \sum_j |\langle \beta | \beta(t) \rangle_j|^2 . \tag{52}$$

The classical analogue of the autocorrelation function is the square root of the classical probability function, illustrated in figure 10. After long times the classical probability function approaches a constant value, which can be found analytically (see appendix C for details) to be

$$P_\beta(\infty) \simeq \frac{3}{2} \sqrt{\frac{\pi}{2}} \frac{\sigma_\beta}{q^\beta} . \tag{53}$$

This analytical result agrees very well with the numerical results, illustrated in figure 10. In the semiclassical autocorrelation, the phases are present and we have a coherent sum which yields the quantum interference between terms

$$|C_\beta(t)|^2 = \left| \sum_j \langle \beta | \beta(t) \rangle_j \right|^2 . \tag{54}$$

Thus, as we have seen in section 6, the reproduction of the recurrences in the autocorrelation function in the semiclassical approximation is due to the principal contributions of the sum adding in phase.

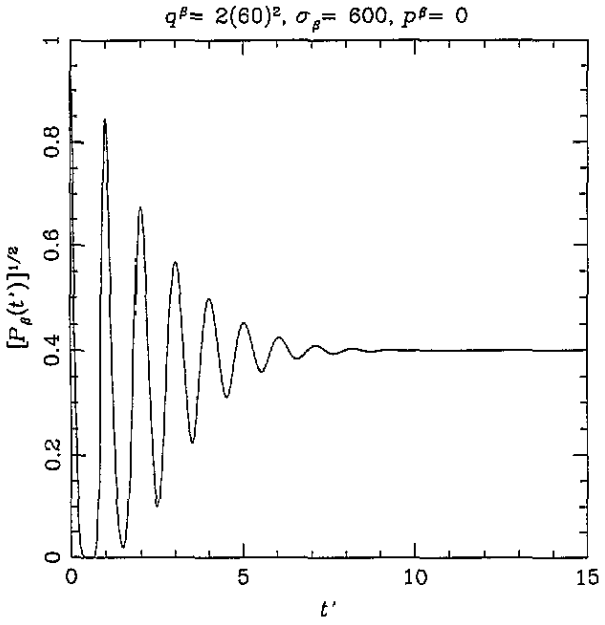

Figure 10. The square root of the classical probability function where $q^\beta = 7200$ and $\sigma_\beta = 600$. The incoherent sum of wave packets causes this function to level off to a constant after long times. The analytic value of this constant found by (53) in this case is 0.3958, which agrees accurately with the figure.

8. Discussion and conclusions

The semiclassical theory presented here incorporates nonlinear dynamics through multiple reference trajectories which are governed by the classical equations of motion. The use of these reference trajectories in some sense explicitly and successfully takes advantage of Feynman's intuitive notion of a classical path. By incorporating the nonlinear classical dynamics correctly, we have demonstrated the long-time accuracy of the semiclassical approximation in the Coulomb potential. However, as one might expect, there are circumstances where this approximation fails. Failure of the semiclassical approximation is expected when the behaviour of the classical motion in the neighbourhood of the reference trajectory is no longer well modelled by linear approximations. In this way, the accuracy of the semiclassical method can be predicted by looking at the behaviour in phase space of the classical analogue. An example of the breakdown of the semiclassical method can be seen in figure 11. In this case the momentum uncertainty is twice that of the previous example, seen in figure 3, which leads to more curvature in the strips of the time evolution of the initial Gaussian wavepacket in phase space. Comparing the semiclassical and exact autocorrelation functions in figures 12 and 13 shows the breakdown of the semiclassical approximation in this particular case.

Our extension of linear wavepacket dynamics to include the use of multiple reference trajectories gives a simple and elegant derivation of semiclassical theory while avoiding the explicit use of the Green-function formalism. Applying the method to the Coulomb potential, we find that the semiclassical approximation is in excellent agreement with a quantum calculation of the autocorrelation function in many circumstances. The semiclassical approximation yields all of the detailed and long-time quantum behaviour including the wavepacket and fractional recurrences, and a remarkable reproduction of the quantum spectrum through a Fourier transform of the semiclassical autocorrelation function. Calculating the Wigner distribution, we find that the classical probability function approaches a constant for long times due to the incoherent sum between the terms for each reference

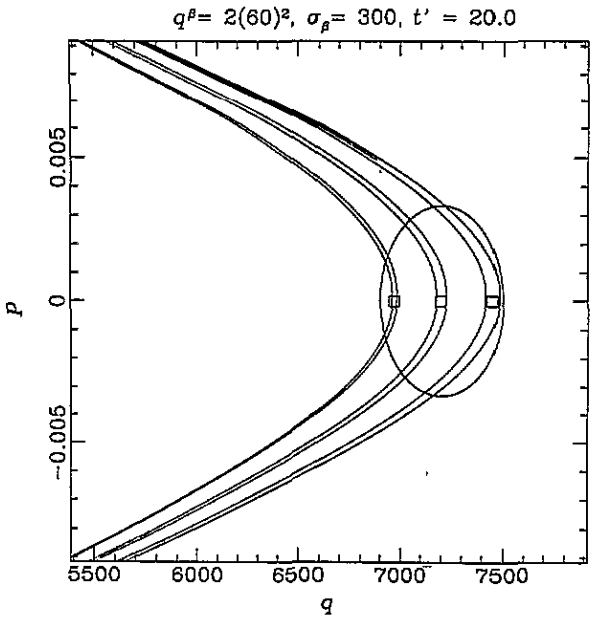

Figure 11. An ellipse in phase space representing the initial Gaussian with parameters $q^\beta = 7200$, $p^\beta = 0$, and $\sigma_\beta = 300$ is propagated classically to a time $t' = 20.0$. The high momentum uncertainty causes the overlap between the initial and propagated wave packets to be not well modelled by linear Gaussian approximations.

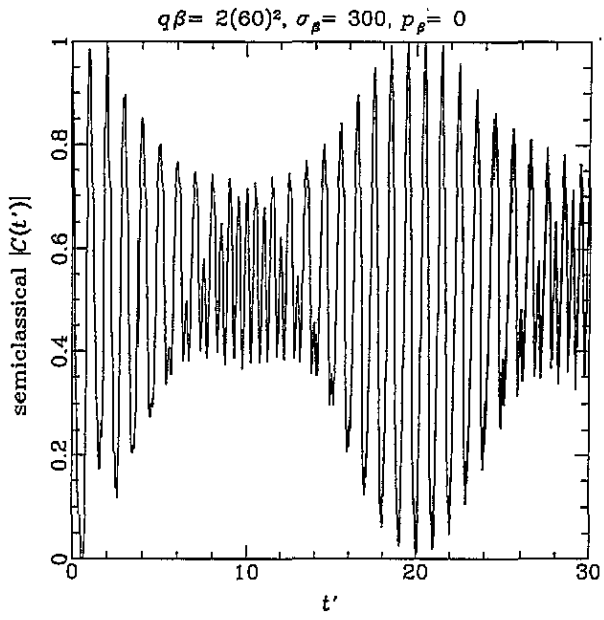

Figure 12. The absolute value of the semiclassical autocorrelation function is shown for long times, where $q^\beta = 7200$ and $\sigma_\beta = 300$. The high momentum uncertainty causes a poor comparison with the exact quantum autocorrelation, shown in figure 13.

trajectory. Thus, we gain the insight that the reproduction of the detailed quantum behaviour in the semiclassical approximation is due to the constructive interference between the terms associated with each reference trajectory. We find that the Coulomb singularity poses no serious problems as long as the end points of the reference trajectories are far away from the origin. Considering the success of the semiclassical approximation of the Coulomb potential, this method promises to be useful in other applications in atomic and molecular physics as well.

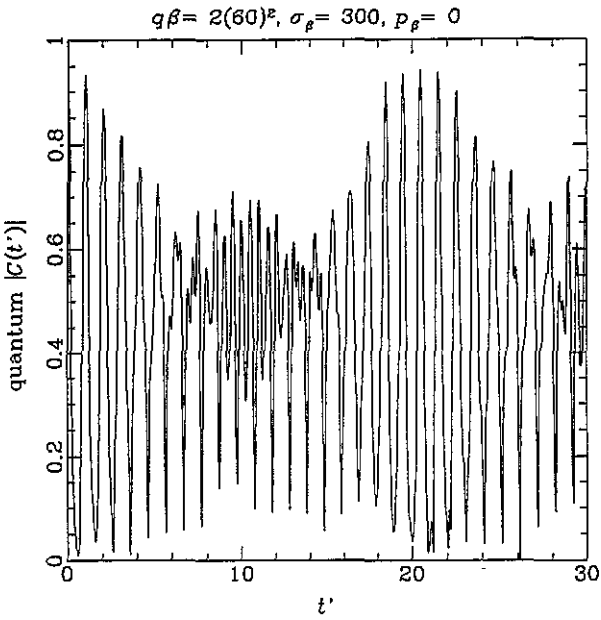

Figure 13. The absolute value of the quantum autocorrelation function is shown for long times, where $q^\beta = 7200$ and $\sigma_\beta = 300$.

Appendix A. Solutions for f and g

In terms of the independent variable θ, g_t satisfies the second-order differential equation (recall (9)),

$$(1-\cos\theta)\frac{\mathrm{d}^2 g}{\mathrm{d}\theta^2} - \sin(\theta)\frac{\mathrm{d}g}{\mathrm{d}\theta} - 2g = 0. \tag{A1}$$

In order to solve this equation, let us think of a nearby trajectory $\hat{q}_t$ which can be approximated by $\hat{q}_t = q_t + \delta q_t$, where $\ddot{\hat{q}}_t = \dot{\hat{p}}_t = -V'(\hat{q}_t)$, and $\ddot{q}_t = \dot{p}_t = -V'(q_t)$. Now, $V'(\hat{q}_t)$ can also be approximated in terms of q_t, therefore $\ddot{\hat{q}}_t = -V'(q_t) - V''(q_t)\delta q_t$, but also $\ddot{\hat{q}}_t = \ddot{q}_t + \delta\ddot{q}_t$. Therefore $\delta\ddot{q}_t = -V''(q_t)\delta q_t$. But this is the same equation (9) that g_t must satisfy. This means that if we solve for δq_t we solve for g_t. Therefore solving for $\delta q_t = (\partial q_t/\partial E)\delta E + (\partial q_t/\partial\theta)\delta\theta$ subject to the constraint $\delta t = (\partial t/\partial E)\delta E + (\partial t/\partial\theta)\delta\theta = 0$ we find two solutions for g_t, one regular solution:

$$g^{(a)} = 1 + \frac{\sin\theta(\sin\theta - 3\theta)}{4(1-\cos\theta)} \tag{A2}$$

and one singular solution:

$$g^{(b)} = \frac{\sin\theta}{1-\cos\theta} \tag{A3}$$

which is proportional to p_t, (recall (22)). Therefore, g_t is a linear combination of these two solutions:

$$g_t = C^{(a)}g^{(a)} + C^{(b)}g^{(b)} \tag{A4}$$

where the constants are determined by the initial conditions. Correspondingly, we have

$$f^{(a)} = \dot{g}^{(a)} = \frac{(2E)^{3/2}}{4(1-\cos\theta)}\left[-\sin\theta + \frac{3(\theta-\sin\theta)}{(1-\cos\theta)}\right] \tag{A5}$$

and

$$f^{(b)} = \dot{g}^{(b)} = -\frac{(2E)^{3/2}}{(1-\cos\theta)^2}\,. \tag{A6}$$

f_t is a linear combination of these last two equations, namely

$$f_t = C^{(a)} f^{(a)} + C^{(b)} f^{(b)}\,. \tag{A7}$$

For this paper we have arbitrarily chosen $g_0 = 1$ as our initial condition. This gives $f_0 = 2\alpha_0 = \mathrm{i}/\sigma\beta^2$ (recall (8)). For our calculations, it is better to write g_t and f_t in terms of q_t and p_t:

$$g_t = \frac{\alpha_0}{E}(2p_0q_t - 2q_0p_t - 3tp_tp_0) + \frac{1}{2q_0^2E}(2q_t - 3tp_t - q_0^2p_0p_t) \tag{A8}$$

$$f_t = \frac{1}{q_t^2E}\left[\alpha_0(3tp_0 + 2q_0 - q_t^2p_tp_0) + \frac{1}{2q_0^2}(3t + p_0q_0^2 - q_t^2p_t)\right] \tag{A9}$$

which are (24) in section 5. In this language, the particular solution $g^{(h)}$ which appears in (14) is

$$g^{(h)} = \frac{1}{2E}(2p_0q_t - 2q_0p_t - 3tp_tp_0) \tag{A10}$$

which is (25), and the action for the Coulomb potential is

$$S = 3Et + 2(q_tp_t - q_0p_0) \tag{A11}$$

which is (26).

Appendix B. Exact quantum calculation

To calculate the autocorrelation function, a Gaussian wavepacket is constructed from the energy eigenstates

$$\psi(x,0) = \sum_{n=1}^{\infty} b_n\psi_n(x) = (\pi\sigma^2)^{-1/4}\exp[-(x-q^\beta)^2/2\sigma^2] \tag{B1}$$

where the expansion coefficients b_n are given by

$$b_n = \int_0^\infty \psi(x,0)\psi_n(x)\,\mathrm{d}x\,. \tag{B2}$$

The time evolution of the wavepacket is then given by

$$\psi(x,t) = \sum_{n=1}^{\infty} b_n\psi_n(x)\ \exp(-\mathrm{i}E_nt) \tag{B3}$$

where E_n are the energy eigenvalues. For the Coulomb potential, the energy eigenvalues are

$$E_n = -\frac{1}{2n^2} \qquad n = 1, 2, 3\ldots \tag{B4}$$

in the units where $\hbar$, the mass, and the strength of the potential are unity. The autocorrelation function is

$$C(t) = \int_0^\infty \psi(x,t)\psi^*(x,0)\,\mathrm{d}x = \sum_{n=1}^{\infty}|b_n|^2\exp(-\mathrm{i}E_nt)\,. \tag{B5}$$

The expansion coefficients b_n are calculated by numerical integration of (B2). Schrödinger's equation for the Coulomb potential can be solved exactly. The normalized energy eigenstates are [40]

$$\psi_n = \left\{ \left(\frac{2}{n}\right)^3 \frac{(n-1)!}{2n(n!)^3} \right\}^{1/2} \left(\frac{2x}{n}\right) \exp(-x/n)\ L_n^1(2x/n) \tag{B6}$$

where L_n^1 are the associated Laguerre polynomials [41]

$$L_n^1(z) = \sum_{m=0}^{n} (-1)^m \binom{n+1}{n-m} \frac{1}{m!} z^m . \tag{B7}$$

The classical turning point for each eigenstate is at $2n^2$. These eigenfunctions are the same as the three-dimensional hydrogen eigenfunctions with zero angular momentum.

For high quantum number n the power series for the Laguerre polynomials in (B7) becomes difficult to compute numerically because of round-off error. For small x, near the singularity in the potential, the power-series solution is computable. Near the classical turning point, where the potential can be approximated as linear, the eigenfunction is approximated by the Airy function which is calculated using a power series [41],

$$\mathrm{Ai}(y) = c_1 F(y) - c_2 G(y) \tag{B8}$$

where $c_1 = 0.355\,028\,053\,887\,817$, $c_2 = 0.258\,819\,403\,792\,807$ and F and G are given by

$$F(y) = \sum_{k=0}^{\infty} 3^k \left(\frac{1}{3}\right)_k \frac{y^{3k}}{(3k)!} \tag{B9}$$

$$G(y) = \sum_{k=0}^{\infty} 3^k \left(\frac{2}{3}\right)_k \frac{y^{3k+1}}{(3k+1)!} \tag{B10}$$

with

$$\left(\beta + \tfrac{1}{3}\right)_0 = 1 \tag{B11}$$

and

$$3^k \left(\beta + \tfrac{1}{3}\right)_k = (3\beta+1)(3\beta+4)\cdots(3\beta+3k-2) \tag{B12}$$

and y is [40]

$$y = \begin{cases} -\left[\frac{3}{2}\int_x^{x_0} \sqrt{2(E - V(x'))}\,\mathrm{d}x'\right]^{2/3} & x < x_0 \\ +\left[\frac{3}{2}\int_{x_0}^{x} \sqrt{2(V(x') - E)}\,\mathrm{d}x'\right]^{2/3} & x > x_0 . \end{cases} \tag{B13}$$

In the region between the Airy function solution and the Laguerre polynomial power-series solution, the eigenfunction is approximated by the standard WKB solution [40]

$$\psi \sim \frac{1}{(E - V(x))^{1/4}} \sin\left(\frac{2}{3}(-y)^{3/2} + \frac{\pi}{4}\right) . \tag{B14}$$

Well beyond the classical turning point the eigenfunction is approximated by the standard WKB solution that exponentially decays to zero.

$$\psi \sim \frac{1}{(V(x) - E)^{1/4}} \exp\left(-\frac{2}{3}y^{3/2}\right) . \tag{B15}$$

The amplitude of the Laguerre polynomial power-series solution is matched to the WKB approximation near the origin. Then, this normalized WKB solution is matched to the Airy function power-series solution close to the classical turning point. Finally, the amplitude of the approximate solution is matched to the decaying WKB approximation beyond the classical turning point.

Appendix C. Long-time behaviour of classical probability

Here we find the limit as $t \to \infty$ of the square of the classical probability function given by the Wigner distribution (52). Starting with (33) we find the absolute square of each individual term. Thus we obtain

$$|\langle\beta|\beta(t)\rangle_j|^2 = \left(\frac{t'^2\tau_\beta^2}{(t'\tau_\beta)^2+\epsilon_\beta j^4}\right)^{1/2} \exp\left\{\frac{-2\epsilon_\beta j^4 q^{[\beta]2}\left[(t'/j)^{2/3}-1\right]^2}{\sigma_\beta^2\left((t'\tau_\beta)^2+\epsilon_\beta j^4\right)}\right\} \tag{C1}$$

where $\epsilon_\beta = 9(\pi\sigma_\beta)^4/64$. Note that for the values which make the semiclassical approximation optimum, $\tau_\beta^2 \simeq \epsilon_\beta$. Note also that only the terms where $t' \simeq j$ for large t' are relevant, that is, give a non-zero value for the exponential. Therefore, in this approximation $\epsilon_\beta j^4 >> t'^2\tau_\beta^2$. Then, we can write

$$P_\beta(t') \simeq \sum_{j=1}^{\infty} \frac{\Delta j}{t'}\frac{\tau_\beta}{\epsilon_\beta^{1/2}}\left(\frac{t'}{j}\right)^2 \exp\left\{\frac{-2q^{[\beta]2}}{\sigma_\beta^2}\left[(t'/j)^{2/3}-1\right]^2\right\} \tag{C2}$$

where we introduce Δj $(= 1)$ to facilitate the next step. Now, in the limit where $t' \to \infty$, we can approximate this sum by the integral

$$\lim_{t'\to\infty} P_\beta(t') = P_\beta(\infty) \simeq \frac{\tau_\beta}{\epsilon_\beta^{1/2}}\int_0^\infty \frac{\mathrm{d}z}{z^2}\exp\left\{\frac{-2q^{[\beta]2}}{\sigma_\beta^2}\left[z^{-2/3}-1\right]^2\right\} \tag{C3}$$

where $z = j/t'$. This integral can be evaluated by using the method of steepest descent. Changing variables to $w = z^{-2/3} - 1$ and integrating, we obtain

$$P_\beta(\infty) \simeq \frac{3}{2}\sqrt{\frac{\pi}{2}}\frac{\sigma_\beta}{q^\beta}, \tag{C4}$$

which is (53).

Acknowledgments

This work was supported by ONR grant N00014-90-J1015. One of the authors (ST) was also supported by the National Science Foundation grants CHE-9014555 and PHY93-05582, and another (IMSB) was also supported by the 1993–94 University of California President's Dissertation Year Fellowship.

References

[1] See for example Maslov V P and Fedoriuk M V 1981 *Semiclassical Approximations in Quantum Mechanics* (Dordrecht: Reidel) English translation
[2] Heller E J 1975 *J. Chem. Phys.* **62** 1544
[3] Littlejohn R G 1986 *Phys. Rep.* **138** 193
[4] Wintgen D and Friedrich H 1986 *Phys. Rev. Lett.* **57** 571
[5] Friedrich H and Wintgen D 1989 *Phys. Rep.* **183** 37
[6] Du M L and Delos J B 1987 *Phys. Rev. Lett.* **58** 1731
[7] Huber D, Heller E J and Littlejohn R G 1988 *J. Chem. Phys.* **89** 2003
[8] Alber G 1991 *Comments At. Mol. Phys.* **26** 47
[9] Zobay O and Alber G 1993 *J. Phys. B: At. Mol. Opt. Phys.* **26** L539
[10] Heller E J 1991 *J. Chem. Phys.* **94** 2723
[11] Tomsovic S and Heller E J 1991 *Phys. Rev. Lett.* **67** 664
[12] Sepúlveda M A, Tomsovic S and Heller E J 1992 *Phys. Rev. Lett.* **69** 402
[13] Tomsovic S and Heller E J 1993 *Phys. Rev. Lett.* **70** 1405

[14] Tomsovic S and Heller E J 1993 *Phys. Rev.* E **47** 282
[15] O'Connor P W, Tomsovic S and Heller E J 1992 *Physica* **55D** 340
[16] Sepúlveda M A and Heller E J *Preprint*
[17] Suárez Barnes I M, Nauenberg M, Nockleby M and Tomsovic S 1993 *Phys. Rev. Lett.* **71** 1961
[18] Nauenberg M 1994 *Proc. Int. Symp. on Coherent States (Oak Ridge 1993)* to be published
[19] Suárez Barnes I M 1994 *Chaos, Solitons and Fractals* in press
[20] Yeazell J A and Stroud C R Jr 1988 *Phys. Rev. Lett.* **60** 1494
[21] Noordam L D, ten Wolde A, Muller H G, Lagendijk A and van Linden van den Heuvell H B 1988 *J. Phys. B: At. Mol. Opt. Phys.* **21** L533
[22] ten Wolde A, Noordam L D, Lagendijk A and van Linden van den Heuvell H B 1988 *Phys. Rev. Lett.* **61** 2099; 1989 *Phys. Rev. Lett.* **40** 485
[23] van Linden van den Heuvell H B, Muller H G and Wolde A ten 1988 *Electronic and Atomic Collisions* (Amsterdam: Elsevier)
[24] ten Wolde A, Noordam L D, Muller H G and van Linden van den Heuvell H B 1989 *Lecture Notes in Physics 339* (Berlin: Springer)
[25] Bowman R M, Dantus M and Zewail A H 1989 *Chem. Phys. Lett.* **161** 297
[26] Gruebele M, Roberts G, Dantus M, Bowman R M and Zewail A H 1990 *Chem. Phys. Lett.* **166** 459
[27] Rosker M J, Rose T S and Zewail A H 1988 *Chem. Phys. Lett.* **146** 175
[28] Alber G, Ritsch H and Zoller P 1986 *Phys. Rev.* A **34** 1058
[29] Parker J and Stroud C R Jr 1986 *Phys. Rev. Lett.* **56** 716
[30] Dačić Gaeta Z and Stroud C R Jr 1990 *Phys. Rev.* A **42** 6308
[31] Yeazell J A, Mallalieu M and Stroud C R 1990 *Phys. Rev. Lett.* **64** 2007; 1991 *Phys. Rev.* A **43** 5153
[32] Meacher D R, Meyler P E, Hughes I G and Ewart P 1991 *J. Phys. B: At. Mol. Phys.* **24** L63
[33] Nauenberg M 1989 *Phys. Rev.* A **40** 1133; 1990 *J. Phys. B: At. Mol. Opt. Phys.* **23** L385
[34] Averbukh I Sh and Perelman N F 1989 *Phys. Lett.* **139A** 449; 1990 *Sov. Phys.–JETP* **69** 464; 1991 *Sov. Phys.–Usp.* **34** 572
[35] Baumert T, Engel V, Röttgermann C, Strunz W T and G Gerber 1992 *Chem. Phys. Lett.* **191** 639
[36] Young L A and Uhlenbeck G E 1930 *Phys. Rev.* **36** 1154
[37] Wigner E P 1932 *Phys. Rev.* **40** 749
[38] Hillery M, O'Connell R F, Scully M O and Wigner E P 1984 *Phys. Rep.* **106** 123
[39] Nauenberg M and Keith A 1992 *Quantum Chaos–Quantum Measurement* ed P Cvitanovic *et al* (Deventer: Kluwer)
[40] Sakurai J J 1985 *Modern Quantum Mechanics* (Reading, MA: Addison-Wesley) pp 104–9, 457–8
[41] Abramowitz M and Stegun I A 1972 *Handbook of Mathematical Functions* (New York: Dover) pp 446, 775